Surface Roughness and Normal Force Effects on the Sliding and Rolling Behavior of POM-H Rolls

Leonhard Kilian Doppelbauer, Philipp Siegfried Stelzer, and Zoltán Major

Abstract Polymer bearings are increasingly used due to their simple mass production and good tribological properties. The current contribution presents a macroscopic study of the effects of surface roughness and normal force on the sliding and rolling behavior of POM-H rolls. The counter-face roughness Ra was varied from 0.01 to 0.5 µm and the normal force from 150 up to 350 N. A polynomial regression model was used to analyze the effects of the two parameters and their interaction. The experiments showed that the coefficient of sliding friction depends strongly on the roughness with a distinct minimum at around 0.1 µm and only slightly on the normal force. In contrast, the coefficient of rolling resistance increases strongly with higher normal forces. From 150 to 350 N the coefficient of rolling resistance doubles in value. The roughness has a minor influence in rolling. The difference between sliding and rolling expresses also in the opposite interaction effects of the roughness and normal forces.

Keywords Polymer · Surface roughness · Sliding · Rolling

1 Introduction

Rolling elements made from various thermoplastic polymers play a major role in modern bearing designs. Polymer rolls can not only be manufactured cost-effectively with large batch production methods like injection molding, but they also offer a variety of other advantages such as corrosion resistance, low weight and self-lubrication [1–4]. For these reasons, plastic bearings are widely used in many practical engineering applications from energy conversion systems to aerospace applications [5–7]. The materials used for polymer bearings are either high-performance polymers such

L. K. Doppelbauer (✉) · P. S. Stelzer · Z. Major
Institute of Polymer Product Engineering, Johannes Kepler University Linz,
Altenbergerstraße 69, 4040 Linz, Austria
e-mail: leonhard.doppelbauer@jku.at
URL: https://www.jku.at/institut-fuer-polymer-product-engineering/

M. Abdel Wahab (ed.), *Proceedings of the 8th International Conference on Fracture, Fatigue and Wear*, Lecture Notes in Mechanical Engineering,
https://doi.org/10.1007/978-981-15-9893-7_54

as polytetrafluoroethylene (PTFE) and polyetheretherketone (PEEK) or engineering polymers such as polyamide (PA) and polyoxymethylene (POM). High-performance plastics are expensive and thus not suitable for mass production. However, POM offers good tribological properties at a moderate price. Therefore, it is widely used for mass production of injection molded components in many tribological applications.

While POM-H homopolymers initially show better short-term mechanical properties (higher stiffness) than copolymers (POM-C), they tend to degrade faster over time. For some applications this could lead to performance reduction fairly quickly. High stiffness and dimensional stability, favorable tribological properties (low friction and wear rate) and moderate creep make POM to an attractive bearing material [6, 8, 9]. Furthermore, it is assumed that POM reveals a pronounced self-lubricating effect which allows low friction coefficients at high loads over a long sliding or rolling time [10].

Naturally, a deeper understanding of the factors that influence the friction process is of prime theoretical and practical importance. Two specific factors that have been discussed intensively in the literature for polymers are surface roughness of the counterpart and normal force. Particularly interesting experimental investigations of these two factors for sliding were carried out by [11–16]. In terms of rolling Harrass et al. [17] provided a comprehensive experimental study of the tribological properties under rolling contact of various thermoplastic polymers. In further consequence, the contact as well as the global and local deformation characteristics of polymer rolls need to be concerned [18, 19].

The objective of this research was a macroscopic study of the effects of surface roughness R_a and normal force F_n on the sliding and rolling behaviour of POM-H rolls. A statistical design of experiments was carried out to analyze the coefficients of sliding friction and rolling resistance by means of polynomial regression models. The regression models help to establish a functional relationship and the interactions between R_a and F_n. The results of this contribution could be helpful in the further development and optimization of rolling bearings made of thermoplastic polymers.

The above experiments were designed distinctly as short-term experiments and we intentionally neglected the long-term effects such as transfer film formation on the counterpart and time dependent viscoelastic deformation of the rolls. However, due to the inherent viscoelasticity of POM-H the rolls reveal creep which results in a macroscopic flattening of the cylindrical surface [18, 19]. This flattening may significantly affect the rolling resistance. For the sake of simplicity this flattening was neglected in the recent study in our short-term experiments. The experimental results made the development of corresponding simulation models possible. We are going to analyze above additional effects in a forthcoming simulation study of the sliding and rolling behavior of the thermoplastic rolls.

2 Experimental

2.1 Material and Specimens

Injection molded cylindrical rolls made of the thermoplastic homopolymer polyoxymethylene POM-H were used in the current study. The elastoplastic material properties were measured according to DIN EN ISO 527-2 [20] with a Young's modulus of 2439 ± 6.4 MPa, a Poisson's ratio of 0.37 ± 0.01 and a yield strength of 83 ± 3.5 MPa. The process induced shrinkage and warpage resulted in a concave shape of the rolls (nominal diameter Ø= 5.90 mm, length = 6.00 mm) with a maximum difference in diameter of 0.04 mm in the middle of the specimen, shown in Fig. 1. The surface roughness value of the rolls was R_a 0.5 µm. The roughness was determined both tactically (MarTalk, Mahr GmbH, Göttingen) and optically (Alicona InfiniteFocus, Alicona Imaging GmbH, Graz) because of measurement difficulties due to the curved white surface. However, the two different methods gave the same results.

The counterparts of the rolls were flat friction tracks with different R_a values ranging from 0.01 to 0.5 µm. Again both tactical and optical methods were used in order to ensure an exact roughness measurement of the counterparts. The roughness values and the used materials for the counterparts are summarized in Table 1. The friction tracks made of tool steel (1.2343) were wire eroded to provide a surface with isotropic friction properties. To realize the glass and steel sheet friction tracks small pieces of these materials were glued onto racks made from tool steel.

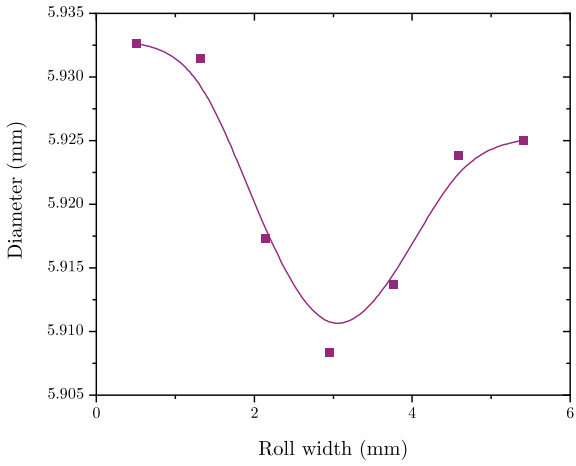

Fig. 1 The profile of the roll diameter shows the volumetric shrinkage caused by the injection molding process. The points correspond to the actual measured values with an approximated spline for better visualization

Table 1 Materials and surface roughness values of the used friction tracks

R_a (µm)	$R_{a,roll}$ / R_a	Materials
0.01	50	Soda-lime glass
0.1	5	Steel (1.2343)
0.15	$3.\dot{3}$	Zinc galvanized sheet steel
0.25	2	Steel (1.2343)
0.5	1	Steel (1.2343)

2.2 Test Setup

All tribological investigations were performed with a UMT Tribolab test rig (Bruker Corporation, Billerica) in a temperature-controlled room at RT 22 ± 1 °C and 50 % rel. humidity. The relative movement between the two friction partners was realized by a linear drive. The normal and tangential forces were measured using a 2D load cell of type DFH-100G with a resolution of 50 mN (Bruker Corporation, Billerica). A system with interchangeable inserts for the friction tracks was developed to enable a quick variation of the surface roughness. These can be mounted on the spring assembly as well as on the carriage by means of a bracket. The spring assembly serves as overload protection for the load cell which is sensitive to impact loads. The schematic structure is shown in Fig. 2 and was extended and modified depending on the test requirements.

A customized measurement script with three main steps was used for the tests. In the first step the test setup moves fast in z direction and stops at 1 mm above the specimen. In the second step the measuring head slowly contacts the roll and builds up the desired radial load. With the parameters shown in Table 2 (left), a targeted overshoot of the contact force is applied to reach the desired load level more quickly as shown in Fig. 3. Since the application of the load is force-controlled, a break-off

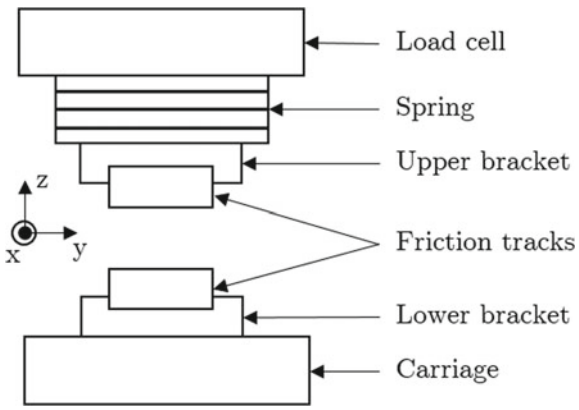

Fig. 2 Schematic structure of the test bench with interchangeable inserts to allow quick variation of the track surface roughness

Table 2 Parameters of the measurement script

Parameter (step 2)	Value	Parameter (step 3)	Value
Touch force	5 N	Load Fz	150/200/250/300/350 N
Pre touch speed	5 mm/s	Speed	10 mm/s
Touch speed	5 mm/s	Displacement in x direction	40 mm
Tracking speed	0.02 mm/s	Data rate	100 Hz
		Cycles	3
		Tracking speed	0.02 mm/s

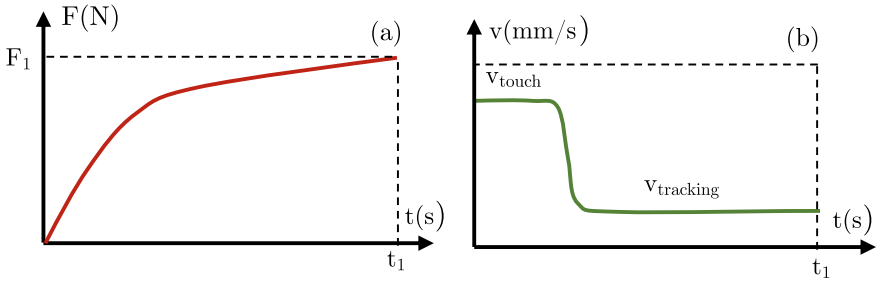

Fig. 3 Load (**a**) and velocity profile (**b**) for the targeted overshoot of the radial load. The time stamp t_1 marks the end of step 2 and the beginning of step 3

condition is introduced in case the test specimen is lost and to prevent a collision of the friction tracks. In the third step the carriage begins to move in x direction and the measurement starts. To exclude transient effects from the measurement the recording of data starts after the third cycle. The parameters of step 3 are shown in Table 2 (right). After finishing the measuring process the test rig moves into home position to enable the withdrawal of the specimen.

2.3 Sliding Test

In the sliding tests, the roll was clamped on one side to prevent the roll from rotating. Therefore, the lower friction track was replaced by a mounting for the roll which essentially consists of an undersized pocket. At the beginning of the sliding test the roll was pressed into this pocket as shown in Fig. 4a. The travel paths were adjusted so that the forward and backward movements do not overlap each other, see Fig. 4b. This was achieved by a lateral offset after the respective forward or backward movement, whereby the measuring head was lifted.

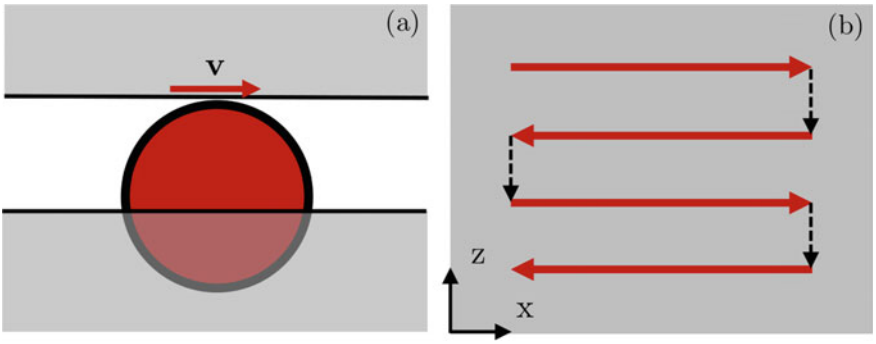

Fig. 4 Roll pressed into an undersized pocket to prevent rolling (**a**), travel path of the measuring head with lateral offset (**b**)

2.4 Rolling Test

For the rolling tests, a single roll was radially loaded between two equal friction plates while the lower plate was moved relatively to the upper one. The translational motion of the lower plate produced the desired rolling motion. To realize a full rotation of the roll the lower plate must move twice the period of the roll curve cycloid which equals to $4\pi R$. Since the actual radius R varies depending on the test specimen, a slightly larger travel distance of the theoretical value was selected for the tests. This ensured that at least one full rotation of the roll was made before the direction of movement was changed in the test.

The roll was aligned with a prism before the start of each experiment to guarantee reproducible results. In that way the roll was always aligned parallel to the rolling direction and the starting position remained the same for each experiment (Fig. 5). The radial load was force-controlled throughout the entire test. The translational movement of the friction tracks are displacement-controlled.

2.5 Test Plan and Data Analysis

In order to be able to detect possible interactions between the different test parameters, a statistical design of experiment as shown in Table 3 was created. Although different materials were used as counter-faces for the friction tracks, they were not evaluated as a separate factor. For each setting (R_a: 0.01–0.5 µm, F_n: 150–350 N), six replicate tests were carried out in sliding. Each sliding test consisted of three partial measurements. For rolling 10 replicate tests were conducted for each testing configuration.

For the data analysis the slight offset of the force signal had to be corrected. In addition, the sections around the reversion of the testing direction were removed to guarantee a constant testing speed. Since the data evaluation works with points and

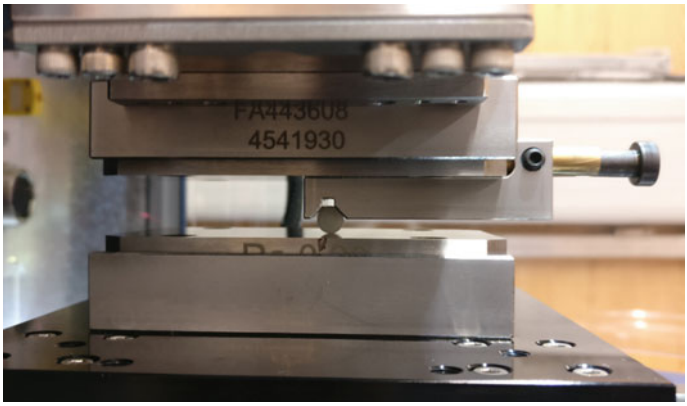

Fig. 5 Roll on a friction track aligned by a prism

Table 3 Experimental design plan for sliding (left) and rolling (right)

R_a (μm)	Sliding (sample size 6)			Rolling (sample size 10)				
	Load F_n (N)			Load F_n (N)				
0.01	150	250	350	150	200	250	300	350
0.1	150	250	350	150	200	250	300	350
0.15	150	250	350	150	200	250	300	350
0.25	150	250	350	150	200	250	300	350
0.5	150	250	350	150	200	250	300	350

their position, the number of points to be removed around the reversal point had to be calculated. Therefore Eq. 1 was used, where v is the testing speed, f the data rate and s the length of the reversal section.

$$Np_{removed}(f, s, v) = \frac{fs}{v} \tag{1}$$

The distance required to overcome the inertia of the test setup after reversing the testing direction was determined experimentally and evaluated for every load level. The tangential force was than calculated as the arithmetic mean of its absolute values. In Fig. 6 a typical signal with its offset and the filtered sections can be seen.

With the values for the tangential and normal force the coefficient of friction μ and the rolling resistance Π were evaluated. With the corresponding values for R_a and F_n as factors a polynomial regression model was fitted (confidence interval 95 %). Polynomial regression functions were chosen due to the good fit in the examined measurement range and to analyze the data with the possible interactions of the parameters. An extrapolation beyond the investigated range is not possible due to the selected approach functions. In order to develop a sufficiently good

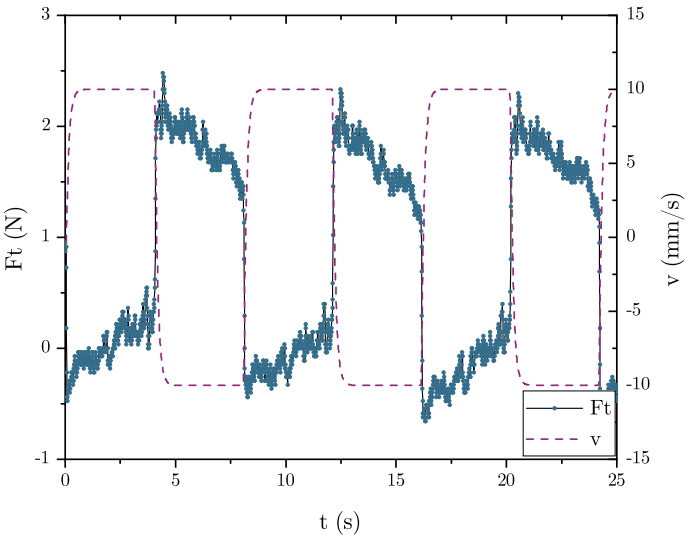

Fig. 6 Typical force signal of a rolling test with the corresponding velocity

model in the test range, polynomial functions up to degree three were used. In contrast, the sum of the powers of the crossed model terms was limited to three (e.g. $f(x, y) = c_j \cdot x^n \cdot y^m | (n + m) \leq 3$).

3 Results and Discussion

3.1 Sliding

The data of the friction coefficient μ depending on the normal force F_n with the roughness R_a as a group parameter are presented in Fig. 7. While the measurements for R_a 0.01 and 0.1 μm show a decreasing trend for μ, the data for v indicates the opposite. In contrast, Fig. 8 shows the dependence on R_a with F_n as group parameter. The values of μ decrease at first but increase again with a distinct minimum at R_a 0.1 μm for all load levels of F_n. This trend is amplified at higher normal forces, possibly due to the deviation from the ideal cylindrical shape of the rolls. The concave shape introduces a concentration of contact at the roll ends. Less contact happens on the side surfaces with only local contacts at roughness peaks. Higher normal forces would lead to more deformation and thus a more even contact distribution along the roll. The same dependency of μ on R_a demonstrated in this work for POM-H was found by the authors of [11] for the polymers PTFE and PE.

The polynomial regression functions (red curve) were used to fit the data and to establish a functional relationship between μ and the parameters R_a and F_n due

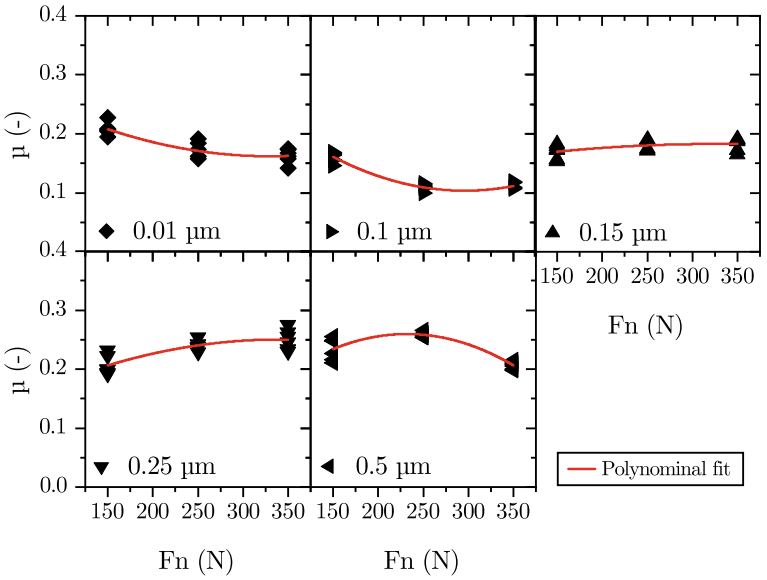

Fig. 7 The friction coefficient μ versus normal force F_n with the surface roughness R_a as group parameter

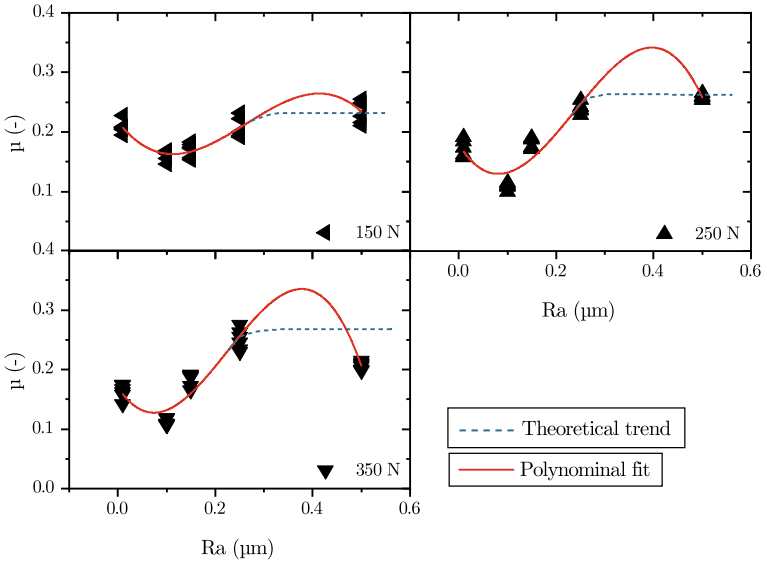

Fig. 8 The friction coefficient μ versus the surface roughness R_a with the normal force F_n as group parameter

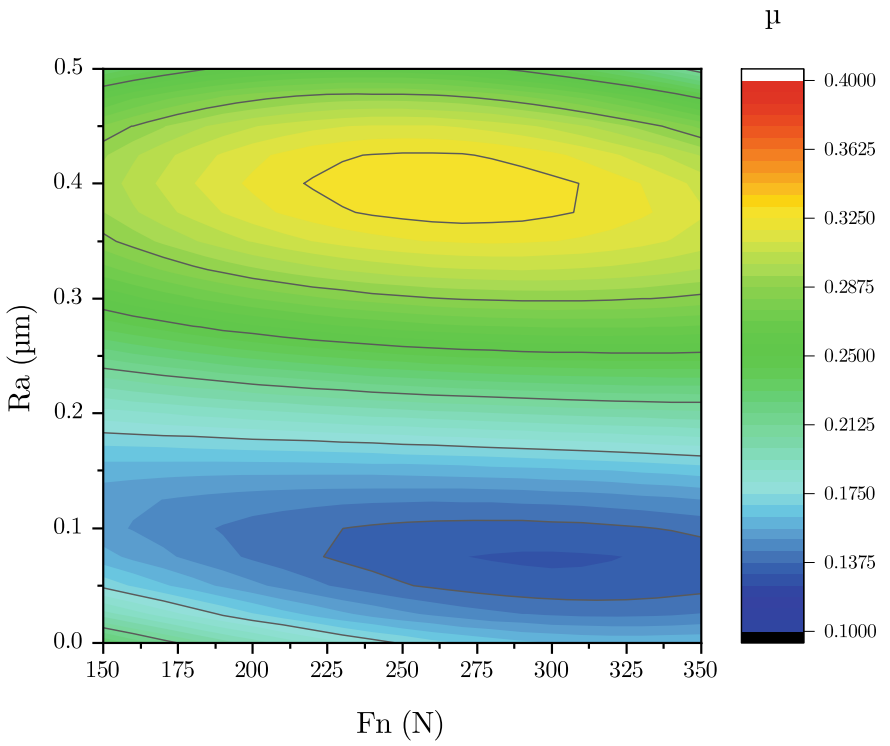

Fig. 9 Contour plot of the regression model for the friction coefficient μ as a function of the normal force F_n and the surface roughness R_a

to the good correlation in the measured test range. However, the local maximum between the measured R_a values of 0.25 and 0.5 μm does not necessarily exist and is rather an artifact of the polynomial functions. Alternatively, the blue line indicates a theoretical trend. We believe that the true trend converges towards a plateau value of μ.

Figure 9 presents the regression model for μ in a contour plot. The polynomial regression model provides a good fit of R-sq. 83.55% for the coefficient of sliding friction. The low gradient in horizontal direction indicates an almost constant influence of F_n. In comparison the influence of R_a is far more pronounced and shows a distinct minimum at around 0.1 μm. The maximum in the contour plot might be an artefact of the used third order functions as discussed above. The gradient of μ in vertical direction changes with the applied load level and clearly indicates an interaction of the two parameters R_a and F_n. These findings offer compelling evidence that the roughness of the counter-face is the dominant factor in the sliding friction of POM-H rolls and that the normal force plays a subordinate role.

3.2 Rolling

The data of the rolling resistance Π depending on F_n with R_a as a group parameter is presented in Fig. 10. It can be easily seen that Π increases strongly for higher values of F_n. The strong influence of the normal force can be traced back to the definition of the rolling resistance. It is strongly related to the contact radius r_c, which is a function of the normal force F_n. The asymmetry of the contact forces during rolling is primarily a cause of the non-linearly increasing contact stresses on the contact surfaces in an ideal cylindrical body. The process-induced concave shape of the roll further complicates the contact problem with non-continuous contact surface and localized stress concentrations at the roll edges.

Figure 11 shows a comparable behavior of the roughness dependency as in the sliding test but with a less distinctive influence of R_a. The curvature slowly decreases and the entire curve is shifted to higher values of Π as the load increases. This indicates an interaction between R_a and F_n as in sliding but in a reciprocal way (compare Figs. 8 and 11). With increasing deformation of the roll this interactional effect decreases and is superposed by the dominating effect of F_n.

Figure 12 displays the polynomial regression model for Π as a contour plot. This regression provides a good fit of R-sq. 95.61%. F_n is the dominant factor with a big horizontal gradient for the rolling resistance. In terms of R_a, as with sliding, a minimum can be found at 0.1 µm which becomes weaker with rising F_n. The flattening of the curve at higher loads is due to the interaction terms of the regression

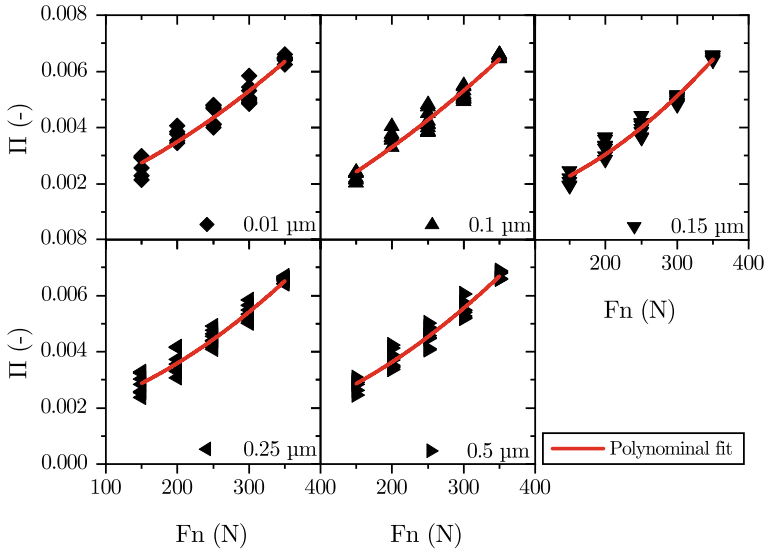

Fig. 10 The coefficient of rolling resistance Π versus normal force F_n with the surface roughness R_a as group parameter

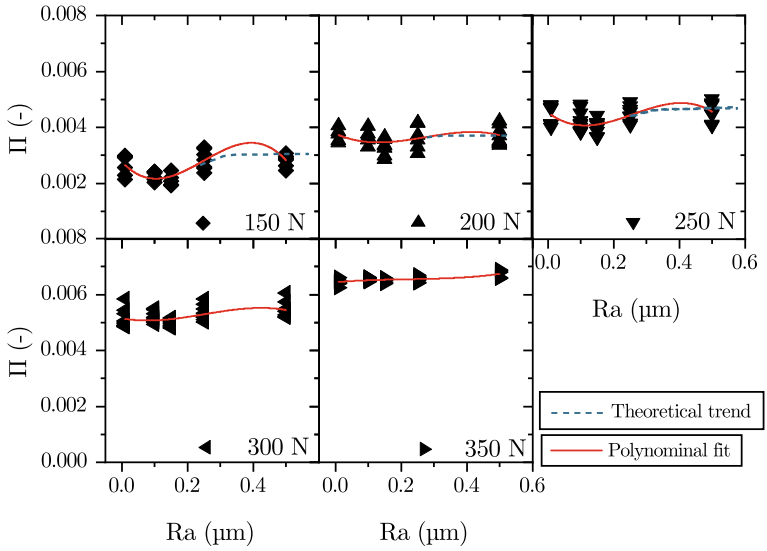

Fig. 11 The friction coefficient Π versus the surface roughness R_a with the normal force F_n as group parameter

model. This effect can be observed particularly well at the two extreme points for the surface roughness (R_a 0.1 µm and 0.4 µm). Contrary to the coefficient of sliding friction, the effect of the normal force dominates over the roughness in rolling. It is likely that the adhesive forces play a minor role than when sliding and thus the lower effect of the surface roughness.

4 Conclusions

The effects of the counter-face roughness R_a and the normal force F_n on the sliding friction µ and rolling resistance Π of POM-H were investigated. The experimental data was analyzed by means of a polynomial regression model to account for possible interactions. The experiments suggest that there is a fundamental difference between sliding and rolling regarding the influence of the roughness and the normal force. While µ was revealed to be strongly affected by R_a but only slightly by F_n, the opposite holds true for the rolling resistance Π. However, the functional relationship of the roughness dependency with a distinct minimum at a R_a value of around 0.1 µm was found to be the same for sliding and rolling.

Furthermore, interactions between the two parameters exist in both cases but they express differently. Based on the curvature of the fits for µ and Π as a function of R_a the interaction with F_n can be illustrated well. On the one hand, the curvature of µ increases with increasing load level; while on the other hand, the curvature of

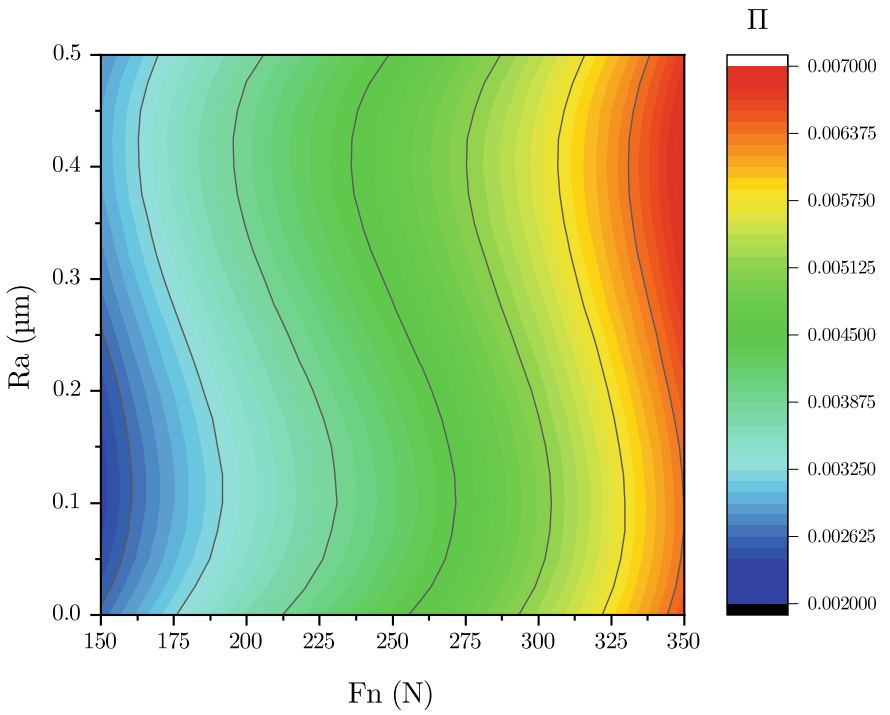

Fig. 12 Contour plot of the regression model for the coefficient of rolling resistance Π as a function of the normal force F_n and the surface roughness R_a

Π decreases. In addition, the entire curve for Π is shifted to higher values when increasing F_n.

Lacking a model based on the underlying physics, it must be emphasized that the polynomial regression was used due to the good correlation in the observed range with a relatively high number of replicate tests (sliding R-sq. 85%, rolling R-sq. 95%). However, the polynomial functions introduce an artificial local maximum between the measured R_a values of 0.25 and 0.5 µm for both sliding and rolling. We believe that the true trend of the friction coefficient and the rolling resistance would converge to a plateau value for higher R_a. Further experiments or a model describing the physics for the influence of the roughness and normal force on the sliding and rolling behavior of polymers are necessary to establish the true functional relationship. Microstructural effects like the transfer film formation and kinetics might explain the interaction between the roughness and normal force on a physical basis.

References

1. Koike H et al (2012) Self-lubrication of PEEK polymer bearings in rolling contact fatigue under radial loads. In: Tribology international, vol 49, pp 30–38. ISSN: 0301-679X. https://doi.org/10.1016/j.triboint.2011.12.005
2. Koike H et al (2012) Observation of crack propagation in PEEK polymer bearings under water-lubricated conditions. In: Machine design and manufacturing engineering, vol 566. Advanced materials research. Trans Tech Publications Ltd, pp 109–114. https://doi.org/10.4028/www.scientific.net/AMR.566.109
3. Berer M, Major Z, Pinter G (2013) Elevated pitting wear of injection molded polyetheretherketone (PEEK) rolls. Wear 297:1052–1063. https://doi.org/10.1016/j.wear.2012.11.062
4. Koike H et al (2013) Observation of wear on PEEK-PTFE hybrid radial bearings. In: Advanced materials and engineering materials II, vol 683. Advanced materials research. Trans Tech Publications Ltd, pp 385–390. https://doi.org/10.4028/www.scientific.net/AMR.683.385
5. Dong Y et al (2015) Design of special plastic bearings and their application in renewable energy conversion system. Open Mater Sci J 9:203–209. https://doi.org/10.2174/1874088X01509010203
6. Samyn P et al (2007) Wear transitions and stability of polyoxymethylene homopolymer in highly loaded applications compared to small-scale testing. In: Tribology international 40(5):819–833. ISSN: 0301-679X. https://doi.org/10.1016/j.triboint.2006.08.003
7. Buck V (1986) Self-lubricating polymer cages for space-proofed bearings: performance and roundness. In: Tribology international 19(1):25–28. ISSN: 0301-679X. https://doi.org/10.1016/0301-679X(86)90091-5
8. Sadık Ünlü B, Atik E, Köksal E (2009) Tribological properties of polymer-based journal bearings. Mater Design 30(7):2618–2622. ISSN: 0261-3069. https://doi.org/10.1016/j.matdes.2008.11.018
9. Benabdallah HS (1997) Reciprocating sliding friction and contact stress of some thermoplastics against steel. J Mater Sci 32(19):5069–5083. https://doi.org/10.1023/A:1018609215248
10. Samyn P, Baets PD (2005) Friction and wear of acetal: a matter of scale. In: Wear 259(1). In: 15th international conference on wear of materials, pp 697–702. ISSN: 0043-1648. https://doi.org/10.1016/j.wear.2005.02.055
11. Tanaka K, Nagai T (1985) Effect of counterface roughness on the friction and wear of polytetrafluoroethylene and polyethylene. In: Ludema KC (ed) Wear of materials, pp 397–404
12. Menezes PL et al (2011) Friction and transfer layer formation in polymer-steel tribo-system: role of surface texture and roughness parameters. In: Wear 271(9). 18th international conference on wear of materials, pp 2213–2221. ISSN: 0043-1648. https://doi.org/10.1016/j.wear.2010.12.047
13. Rojsatean J et al (2017) Friction characteristics of self-lubricating ABS under different surface roughnesses and temperatures. In: Tribol Int 109:229–237. ISSN: 0301-679X. https://doi.org/10.1016/j.triboint.2016.12.055
14. Panda S, Sarangi M, Roy Chowdhury SK (2019) Examinations on PEEK wear debris accumulation over counter surfaces in room and vacuum sliding environments. Polym Test 77:105880. ISSN: 0142-9418. https://doi.org/10.1016/j.polymertesting.2019.04.027
15. Quaglini V et al (2009) Influence of counterface roughness on friction properties of engineering plastics for bearing applications. Mater Design 30(5):1650–1658. ISSN: 0261-3069. https://doi.org/10.1016/j.matdes.2008.07.025
16. Chen W et al (2020) Effect of load on the friction and wear characteristics of Si3N4-hBN ceramic composites sliding against PEEK in artificial seawater. Tribol Int 141:105902. ISSN: 0301-679X. https://doi.org/10.1016/j.triboint.2019.105902
17. Harrass M, Friedrich K, Almajid AA Tribological behavior of selected engineering polymers under rolling contact. Tribol Int 43(3):635–646. ISSN: 0301-679X. https://doi.org/10.1016/j.triboint.2009.10.003. http://www.sciencedirect.com/science/article/pii/S0301679X0900303X

18. Berer M, Major Z (2010) Characterization of the global defor- mation behavior of engineering plastics rolls. Int J Mech Mater Design 6:1–9. https://doi.org/10.1007/s10999-010-9111-9
19. Berer M, Major Zoltan (2012) Characterisation of the local deformation behaviour of engineering plastics rolls. Strain 48:225–234. https://doi.org/10.1111/j.1475-1305.2011.00816.x
20. EN ISO 527-2:2012 Plastics—determination of tensile properties—part 2: test conditions for moulding and extrusion plastics (ISO 527-2:2012); German version EN ISO 527-2:2012. 6-2012. https://doi.org/10.31030/1860304